

Supplementary Materials for  
**BRCA2-HSF2BP oligomeric ring disassembly by BRME1 promotes  
homologous recombination**

Rania Ghouil *et al.*

Corresponding author: Sophie Zinn-Justin, [sophie.zinn@cea.fr](mailto:sophie.zinn@cea.fr); Alex N. Zelensky, [a.zelensky@erasmusmc.nl](mailto:a.zelensky@erasmusmc.nl);  
Roland Kanaar, [r.kanaar@erasmusmc.nl](mailto:r.kanaar@erasmusmc.nl)

*Sci. Adv.* **9**, eadi7352 (2023)  
DOI: 10.1126/sciadv.adi7352

**The PDF file includes:**

Figs. S1 to S9  
Tables S1 to S3  
Legend for data S1

**Other Supplementary Material for this manuscript includes the following:**

Data S1

**Supplementary Fig. S1**

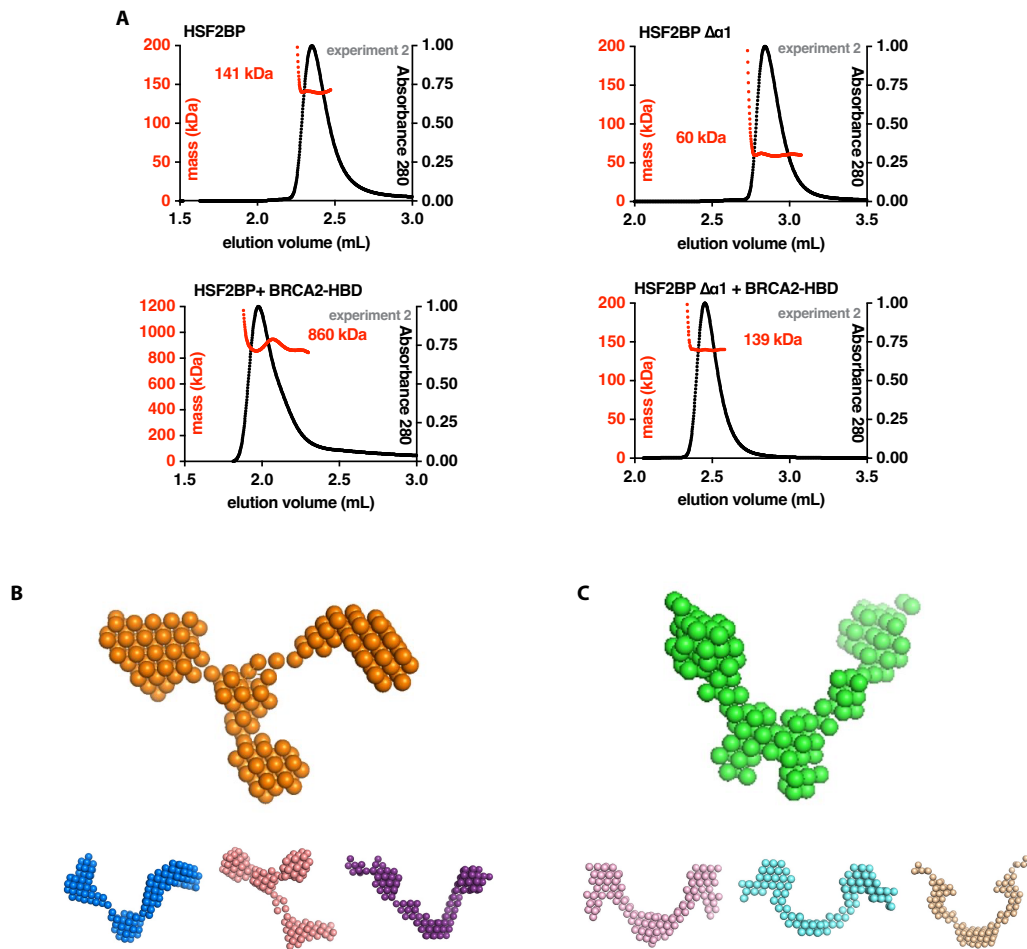
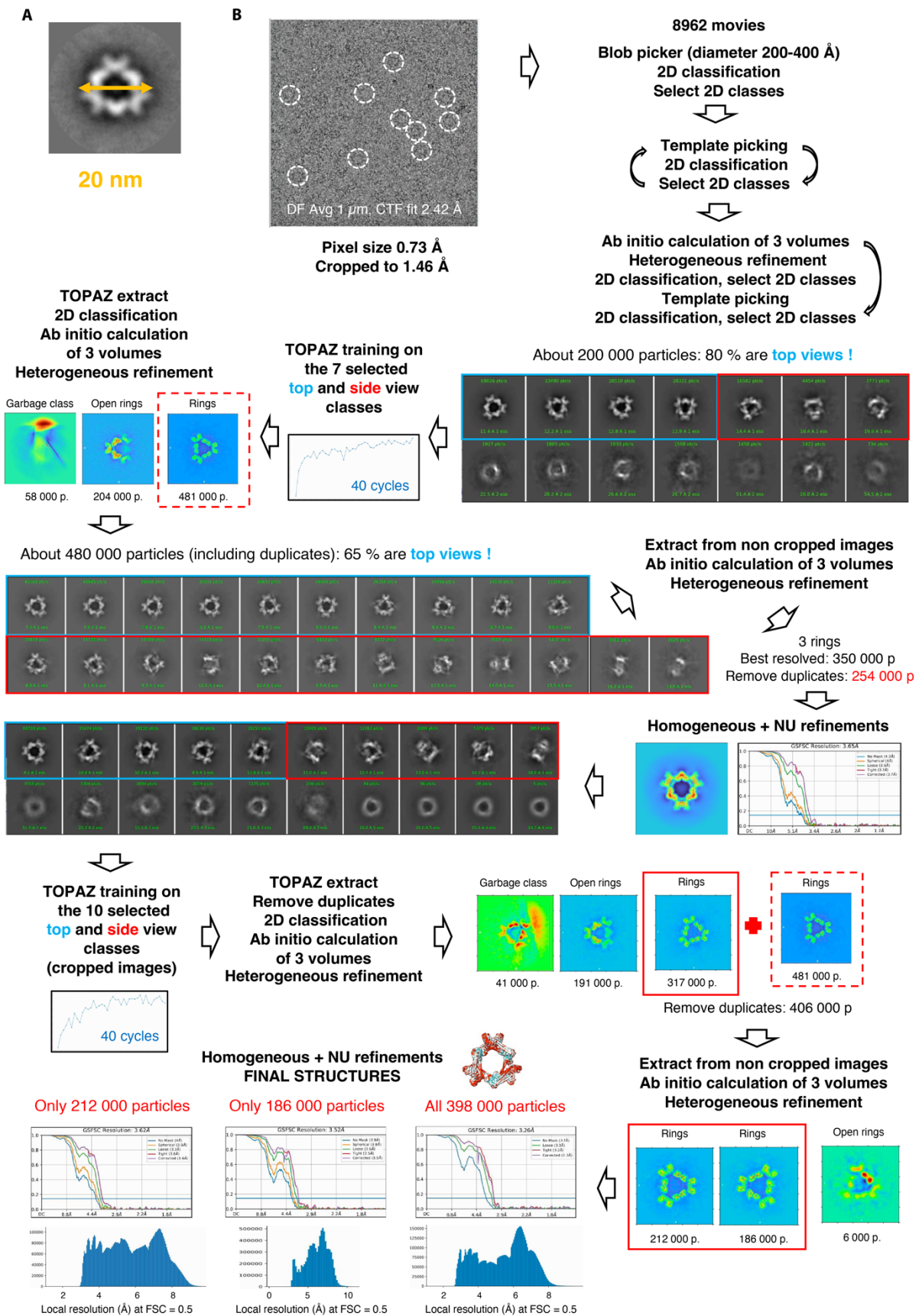


**Fig. S1. Extended data for the SEC-MALS and SEC-SAXS analyses shown in Fig. 1. (A)** SEC-MALS analyses performed on HSF2BP either full-length or lacking helix  $\alpha 1$  (HSF2BP fragment from G48 to V334), when free or bound to BRCA2-HBD. The SEC column is a BIOSEC 3 (Agilent). HSF2BP  $\Delta\alpha 1$  fragment is dimeric (theoretical mass of the dimer: 64 kDa) and assembles as a tetramer when bound to BRCA2-HBD (theoretical mass of the 4:2 complex: 142 kDa). **(B,C)** Models of full-length HSF2BP calculated using the program DAMMIF from the SEC-SAXS data. B, Models calculated without making any hypothesis on the symmetry of the HSF2BP oligomer structure. C, Models calculated by hypothesizing that the oligomer structure has a 2-fold symmetry, as it is formed from two dimers. In both cases, 10 models were calculated. The upper panels show the average models. The lower panels display three representative models.

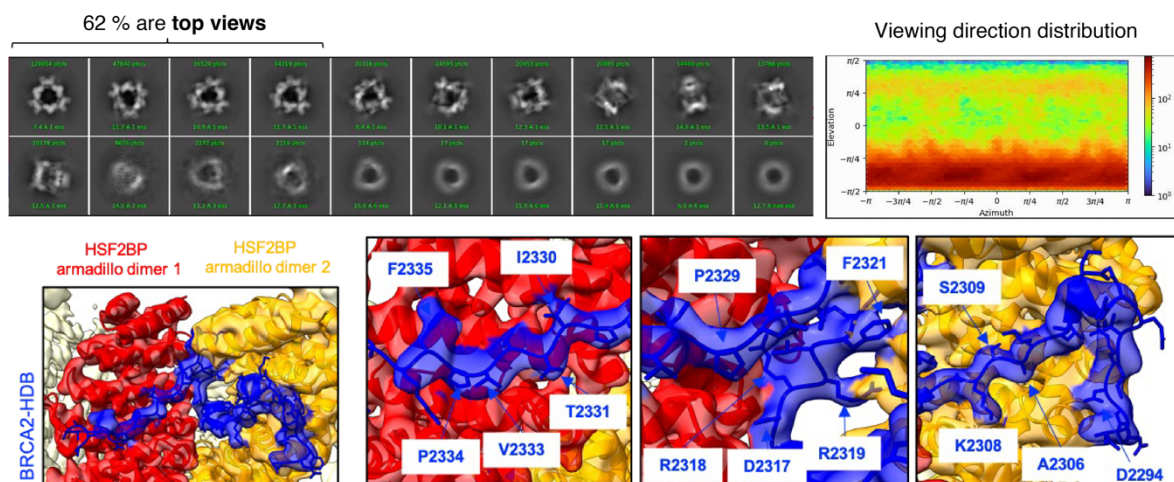
**Supplementary Fig. S2**



(continued on the next page)

Supplementary Fig. S2 (continued)

C FINAL STRUCTURE CALCULATED FROM 398 000 particles WITH A D3 SYMMETRY



D CLASSIFICATION OF THE 398 000 PARTICLES INTO TWO SETS

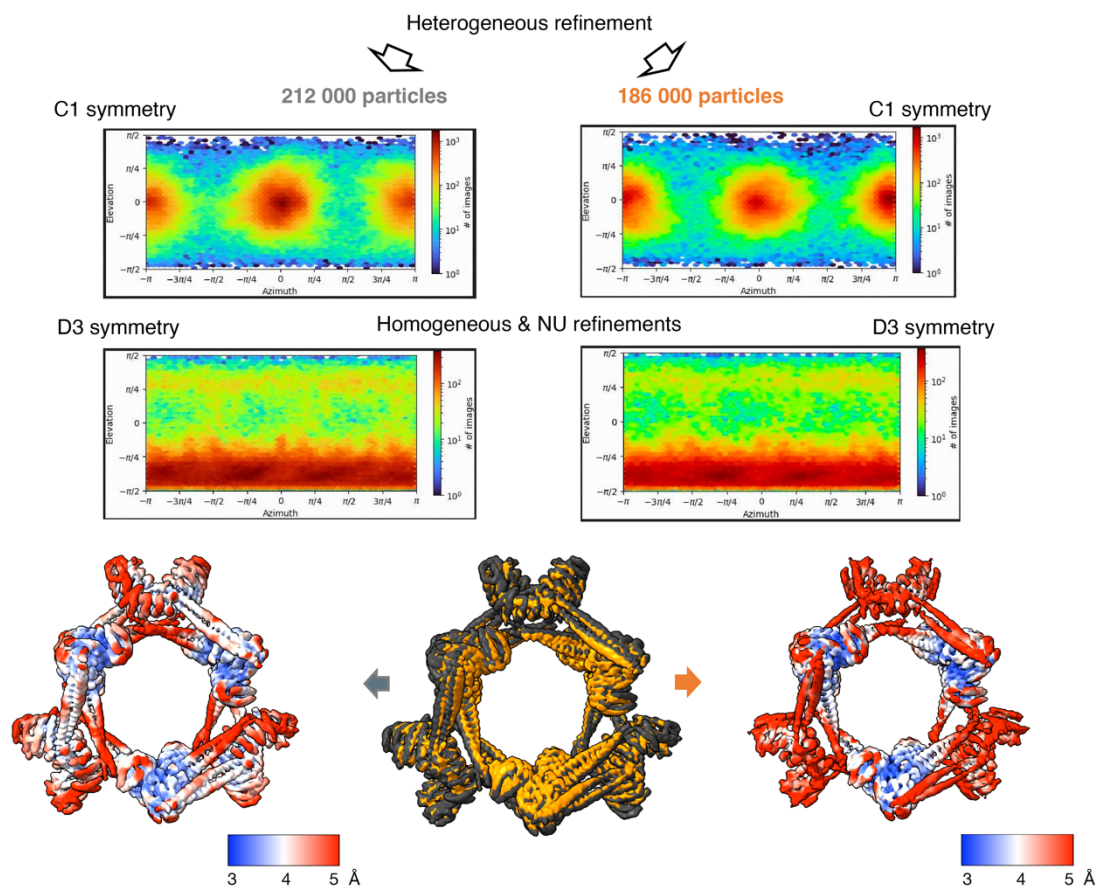




**Fig. S2. Extended data for the cryo-EM analysis shown in Fig. 2.** (A) A typical 2D class obtained from the analysis of negative-staining images recorded on full-length HSF2BP bound to BRCA2-HBD. (B) Flow chart of the processing of the cryo-EM data recorded on HSF2BP bound to BRCA2-HBD. The whole analysis was performed using CryoSPARC. The first TOPAZ calculation provided more side views of the complex, whereas the second TOPAZ calculation provided more particles. At the end, about 44 particles were picked in average on each micrograph. The best resolved volume was obtained from  $8962 \times 44,4 = 398\ 000$  particles (see panel C). Two other volumes were obtained after 3D classification of the 398 000 particles (see panel D). (C) Analysis of the final map calculated from 398 000 particles. 2D classes and viewing direction distribution of the particles are presented. Docking of the crystal structure (7BDX) of the complex formed by four armadillo domains of HSF2BP (first and second armadillo dimers in red and orange, respectively) and two BRCA2-HBD peptides (in blue) into the cryo-EM map is illustrated in the lower panels. The armadillo domains are displayed as cartoons, whereas the BRCA2 peptide is displayed in sticks. The map is colored as the fitted crystal structure. The different zoom views highlight that the BRCA2-HBD peptides nicely fit into the cryo-EM map after docking of the HSF2BP armadillo domains. Well-resolved BRCA2 side chains are marked. (D) Analysis of the cryo-EM maps obtained after classification of the 398 000 particles. The first cryo-EM map, calculated from 212 000 particles (left and grey), has a larger diameter and its resolution is regularly distributed between 3 and 8 Å (see panel B). The second cryo-EM map, calculated from 186 000 particles (right and orange), has a slightly smaller diameter; its inner armadillo domains are better defined, whereas the outer armadillo domains as well as the coiled-coil regions are poorly resolved.

**Supplementary Fig. S3**

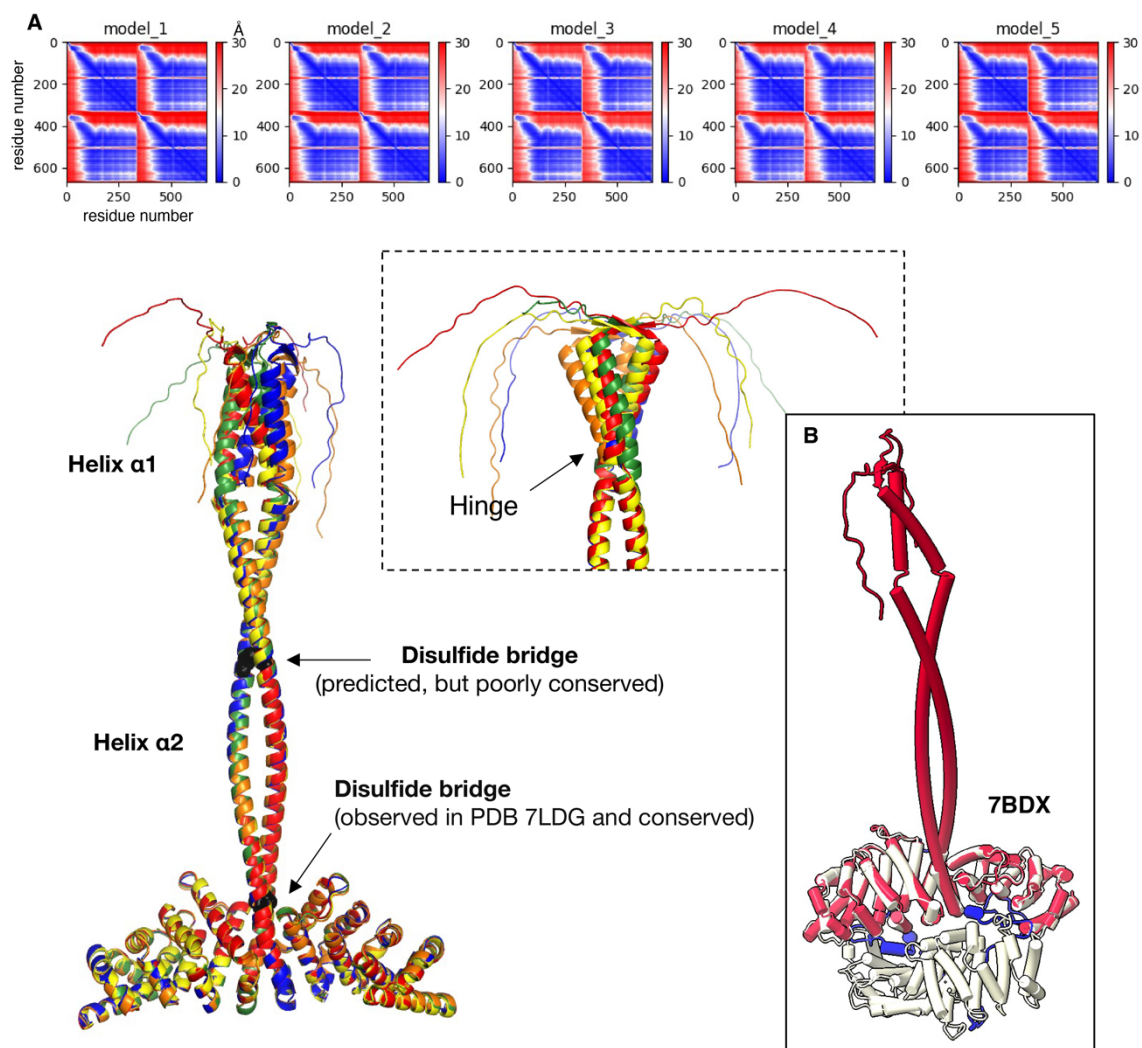


**Fig. S3. Extended data for the AlphaFold analysis of the HSF2BP dimer presented in Fig. 3.** (A) Five models of the HSF2BP dimer calculated by AlphaFold. In the upper panels are displayed the heat maps showing the predicted relative position error (in Å) calculated by AlphaFold between all pairs of residues (HSF2BP residues from the first and second monomers are numbered as 1-334 and 335-668, respectively). The blue color observed in regions corresponding to intermolecular distances proves that the relative position of the two monomers is predicted with high confidence. In the lower panels, the 5 models are superimposed, each of them being displayed in a different color. They all exhibit the same secondary structure elements. Moreover, their 3D structures are identical, except for the position of the disordered N-terminal region (residues 1 to 19), the  $\beta$ -strand (residues 20 to 24), the first helix  $\alpha$ 1 (residues 25 to 45) and the loop between  $\alpha$ 1 and  $\alpha$ 2 (or hinge; residues 46 to 47), as shown in the main panel and in the zoom view rotated by 90° in the dashed boxed panel. Two putative intermolecular disulfide bridges are displayed in black dots in the main panel. (B) Superimposition of one of the AlphaFold models of the full-length HSF2BP dimer (in red) onto the crystal structure of the complex between two HSF2BP armadillo dimers (white) and two BRCA2-HBD peptides (blue) (PDB: 7BDX). (*continued on the next page*)

**Supplementary Fig. S3 (continued)**

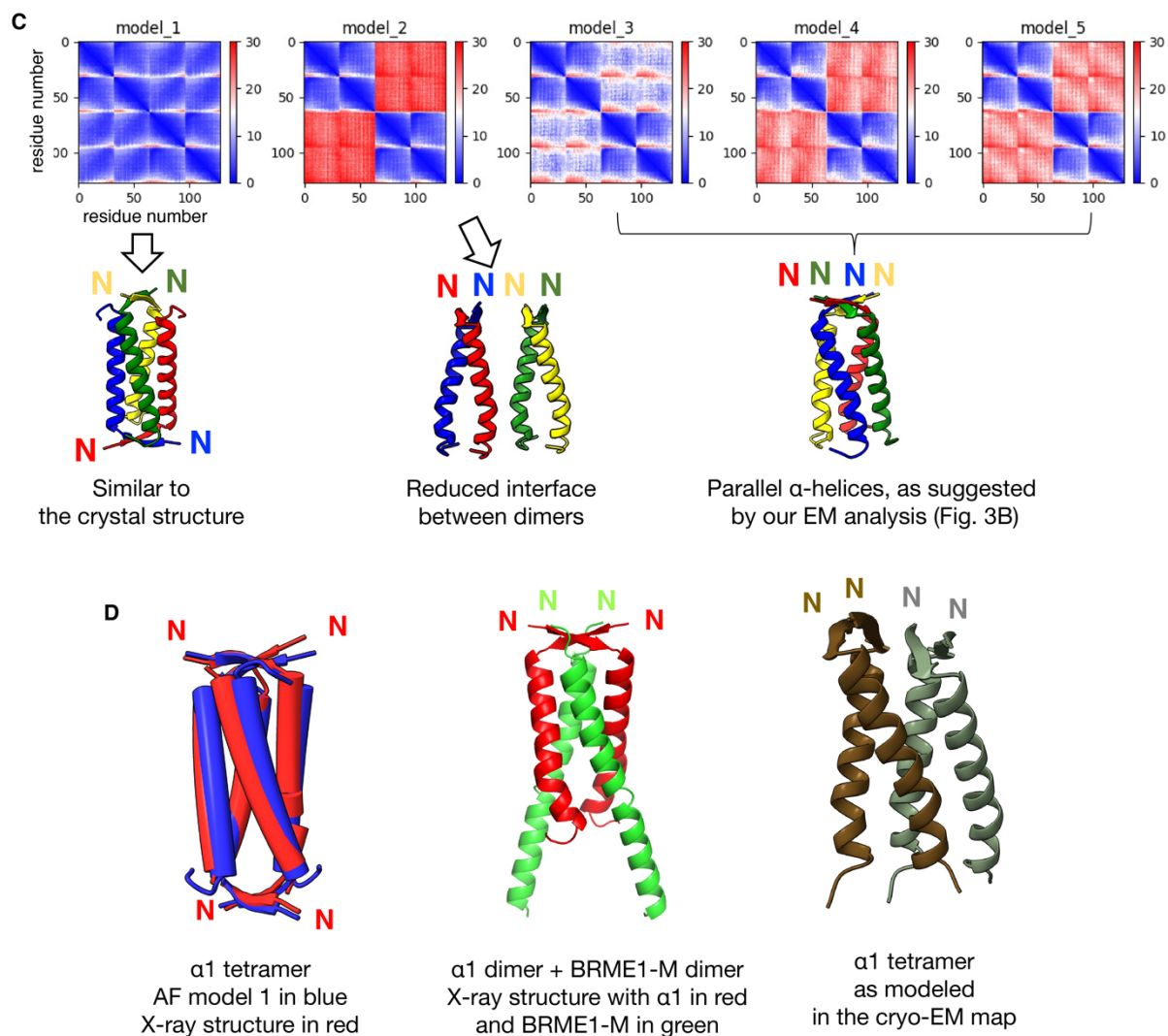


**Fig. S3 (continued)** (C) Five models of the helix  $\alpha$ 1 tetramer calculated by AlphaFold. (D) Analysis of the similarities between the AlphaFold models and the structures/models of the homo- and hetero-tetramers of HSF2BP helix  $\alpha$ 1 and BRME1-M. In the left panel, the AlphaFold model 1 (blue) and our crystal structure of the  $\alpha$ 1 tetramer (red) are superposed ( $C\alpha$  RMSD 0.96 Å). In the middle panel, the crystal structure of two molecules of HSF2BP  $\alpha$ 1 (red) bound to two molecules of BRME1-M (green) is presented for comparison. In the right panel, our model of the  $\alpha$ 1 tetramer, as fitted in the cryo-EM map of the HSF2BP / BRCA2-HBD complex, is displayed. Colors indicate the  $\alpha$ -helices belonging to the same HSF2BP dimer (dimer 1: brown; dimer 2: grey). The  $\alpha$ -helices are all parallel, as in AlphaFold models 2 to 5.

**Supplementary Fig. S4.**

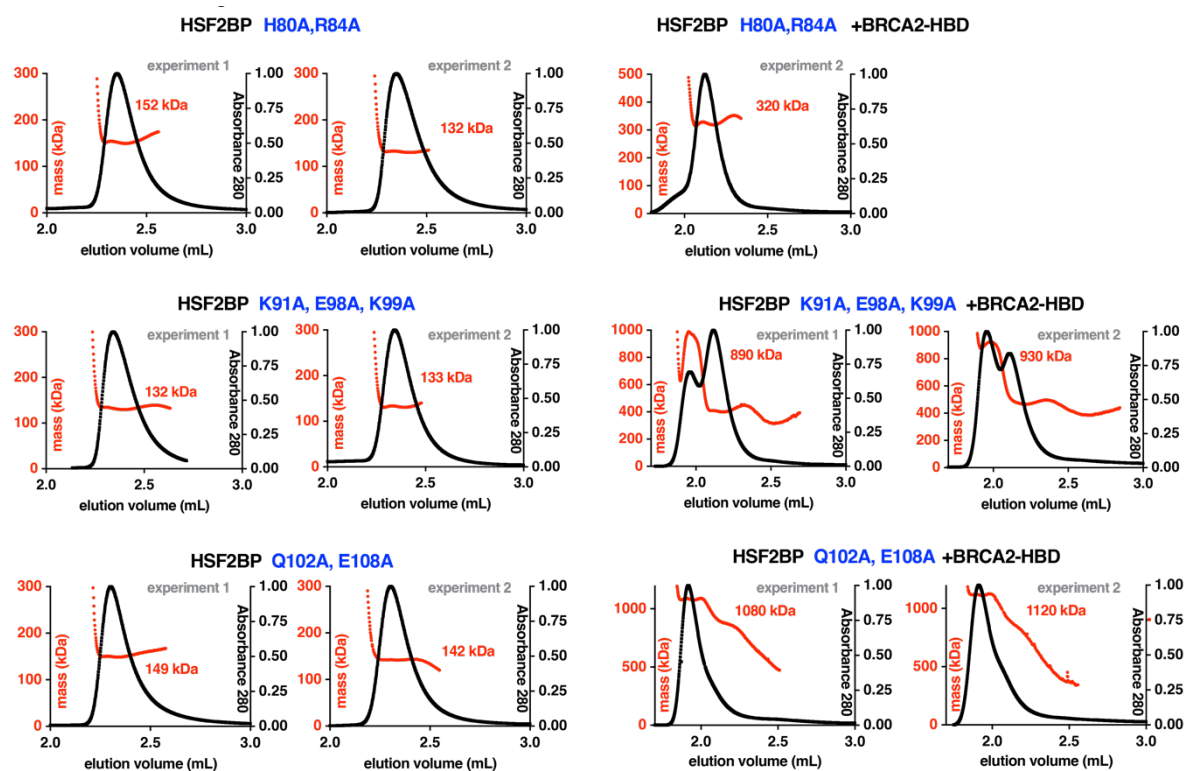


**Fig. S4. Extended data for the SEC-MALS analysis presented in Fig. 3.** Replicate of the experiment shown in Fig. 3D and analyses of other HSF2BP variants with substitutions in the residues that appear to be at  $\alpha 2$ - $\alpha 2$  and  $\alpha 2$ -armadillo interfaces in the cryo-EM model (Fig. 3C). Proteins were analyzed alone and in complex with BRCA2-HBD, experiments were done twice. Predicted molecular weight of the tetrameric HSF2BP is 150 kDa; the 4:2 complex with BRCA2-HBD — 164 kDa; the 8:4 complex — 328 kDa; the 24:12 complex — 984 kDa.



**Supplementary Fig. S5.**

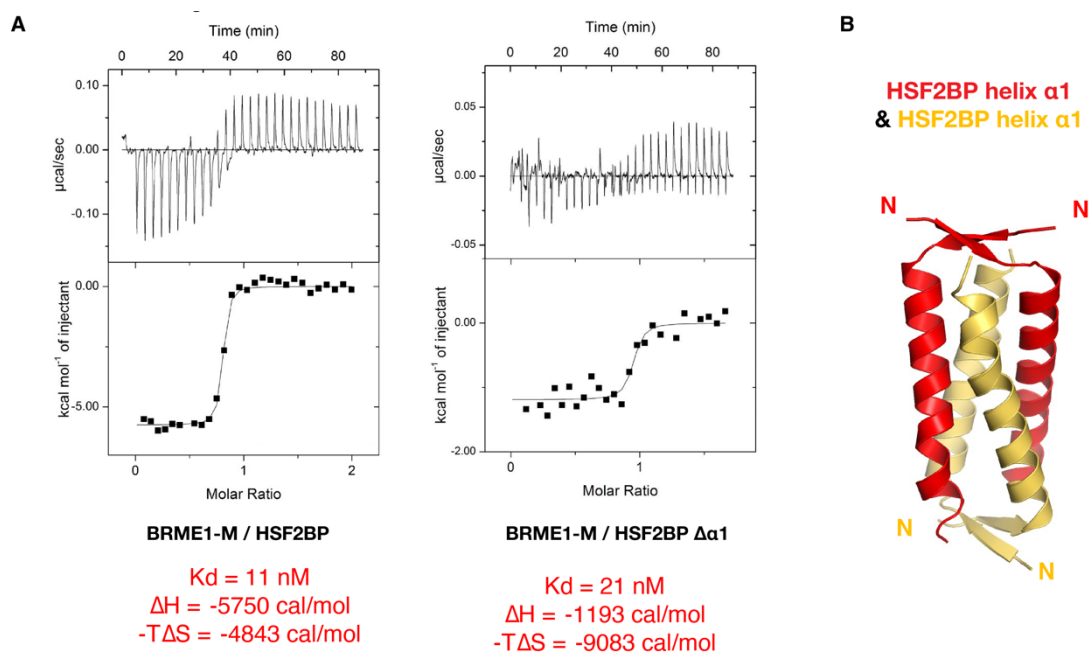


**Fig. S5. Extended data for the biophysical analyses presented in Fig. 4. (A)** Binding of BRME1-M to full-length HSF2BP (left) or HSF2BP helix  $\alpha 1$  (right), as analyzed by ITC at 20°C. A large decrease of the binding enthalpy is observed when comparing the affinity of BRME1-M against HSF2BP helix  $\alpha 1$  versus full length HSF2BP. Such a decrease is not observed at 30°C, as shown in Fig. 4B. All these data are summarized in Table 1. **(B)** Crystal structure of the  $\alpha 1$  tetramer. The HSF2BP peptide E19-V50 is organized as a parallel dimer (each dimer is displayed in red and yellow, respectively), and two of these dimers are interacting in an anti-parallel manner to form the final tetramer. Such conformation was also found by AlphaFold (see Fig. S3C). Whether it can exist in full-length HSF2BP is yet unclear. However, our cryo-EM analysis strongly suggests that it does not exist in the complex between full-length HSF2BP and BRCA2-HBD.

**Supplementary Fig. S6**

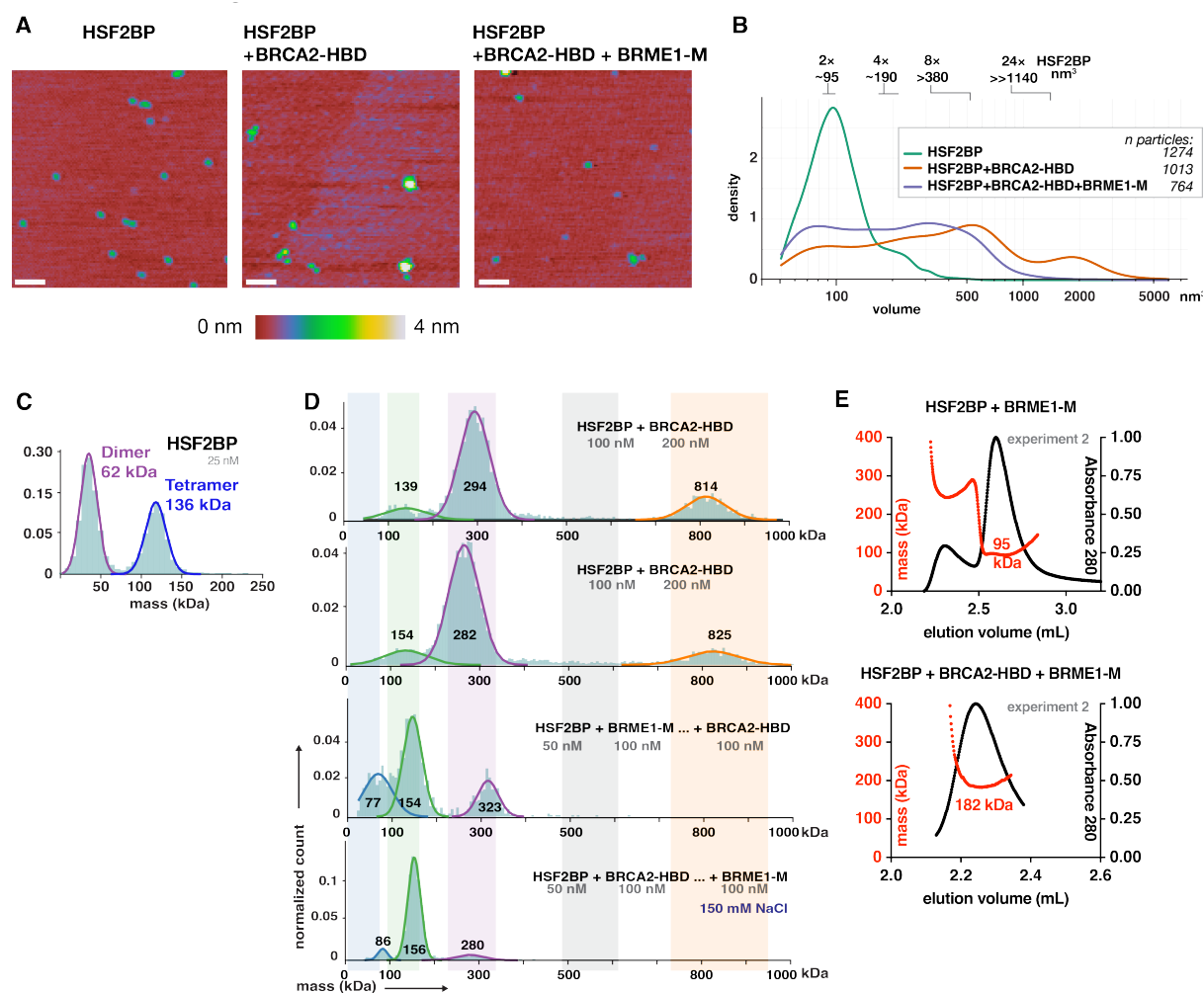


**Fig. S6. Replicates for SFM, mass photometry and SEC-MALS experiments shown in Fig. 5. (A,B)** Representative SFM scan images (scale bar = 100 nm) and corresponding density of volumes distributions of the HSF2BP, HSF2BP+BRCA2-HBD and HSF2BP+BRCA2-HBD+BRME1-M complexes. **(C)** Mass photometry analysis of free HSF2BP at 25 nM (see Fig. 4E). **(D)** Mass photometry analysis of HSF2BP + BRCA2-HBD + BRME1-M to complement experiments shown in Fig. 5E. Top two graphs: replicates of the experiment shown in Fig 5E but at higher concentration (100 nM). Third graph: order of addition was changed by adding BRME1-M 30 min before BRCA2-HBD. Bottom graph: complexes were formed at a lower salt concentration (150 mM NaCl). **(E)** SEC-MALS analyses of the HSF2BP-BRME1 complex in the absence (top panel; 1:1 complex theoretical mass: 42 kDa) or in the presence (bottom panel; 2:2:1 complex theoretical mass: 91 kDa) of BRCA2-HBD.

**Supplementary Fig. S7**

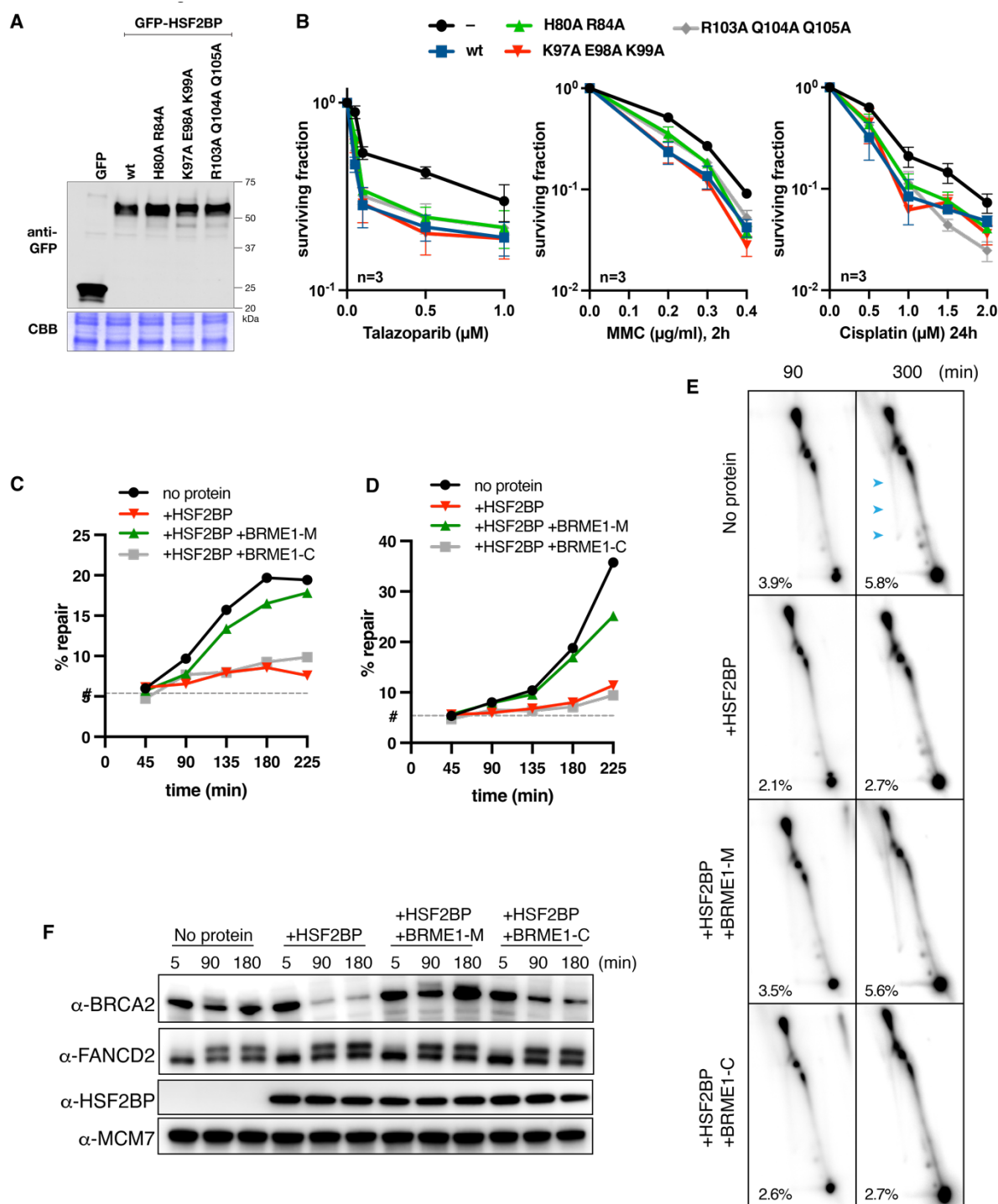


**Fig. S7. Extended data for experiments presented in Fig. 6.** (A) Anti-GFP immunoblot of the total protein extract from HeLa cells stably producing GFP-HSF2BP variants or GFP. (B) Clonogenic survivals of HeLa cells stably producing the indicated GFP-HSF2BP variants or GFP. Surviving fraction after treatment with the indicated concentrations of mitomycin C (MMC), cisplatin or talazoparib is plotted on a log scale. Each experiment was repeated three times, means and s.e.m. are displayed. (C,D) Replicates of the cisplatin crosslink repair assay shown in Fig. 6F. (E) Replicate of the 2D gel electrophoresis of HR intermediates shown in Fig. 6G. (F) Replicate of the immunoblot experiment shown in Fig. 6H.

**Supplementary Fig. S8**

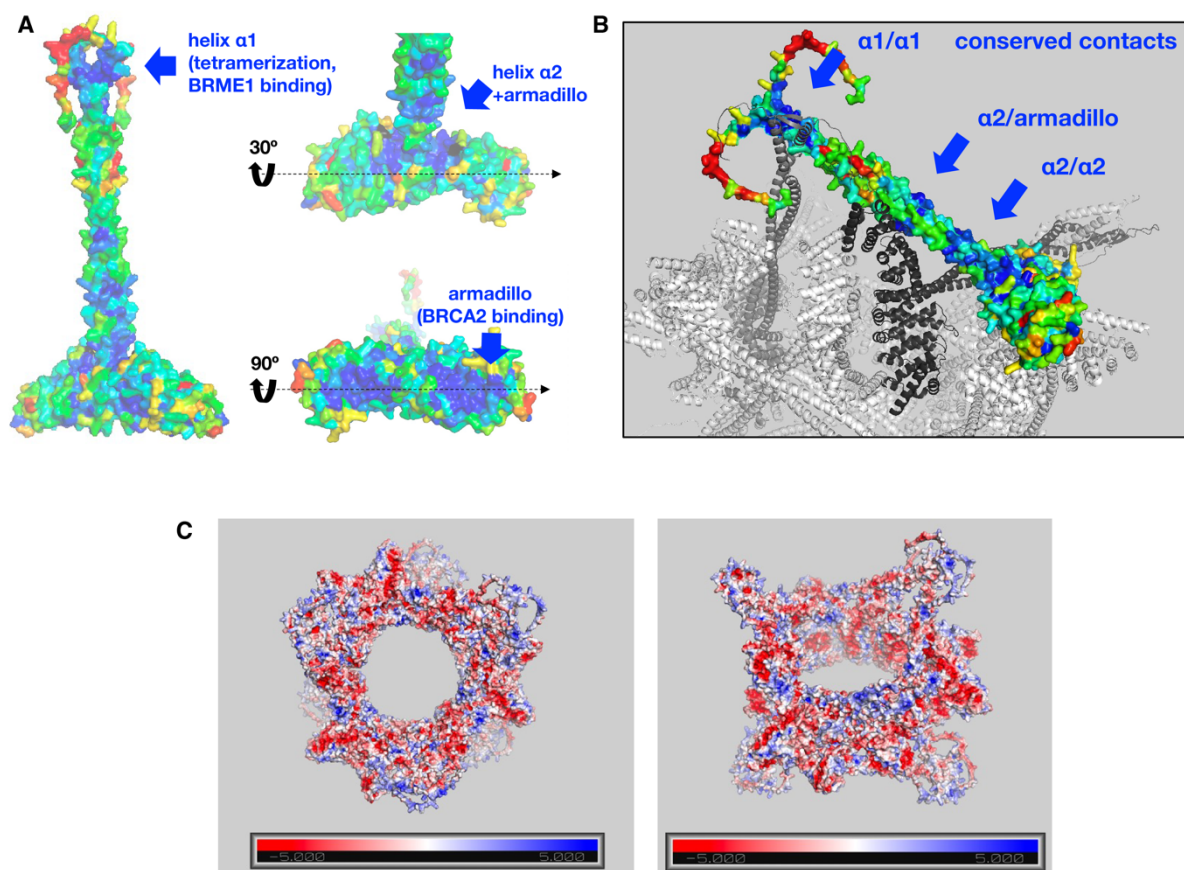
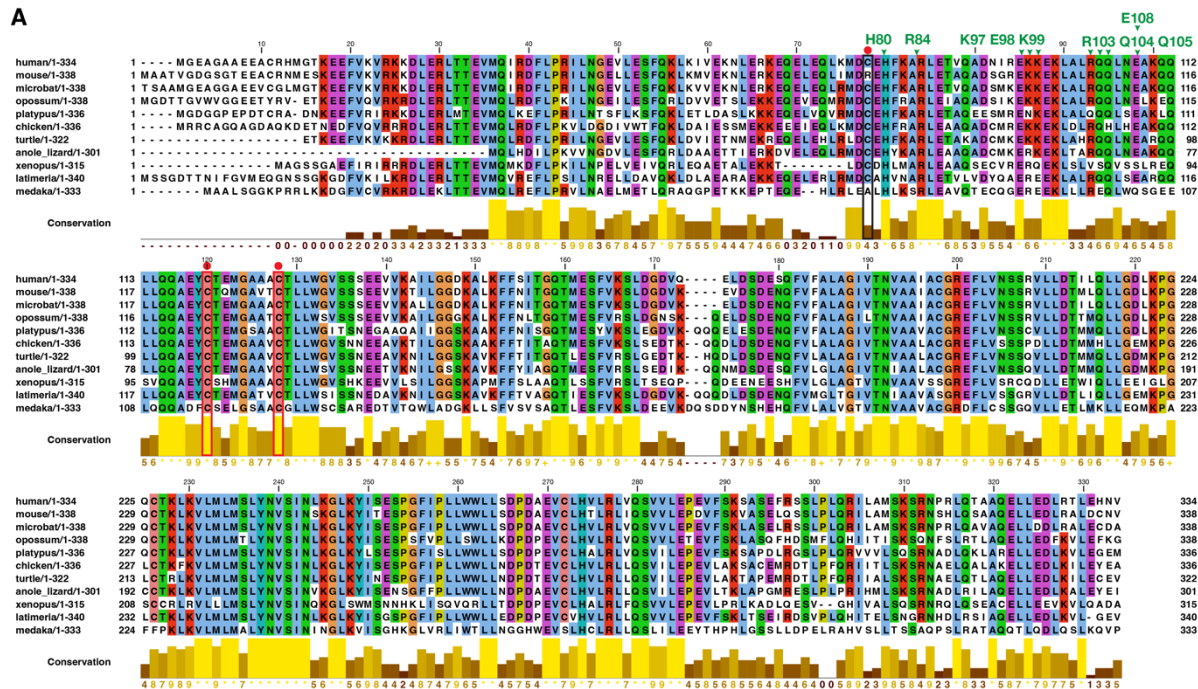


**Fig. S8. Analysis of the surface properties of HSF2BP.** (A) Different views of the surface of the HSF2BP dimer, as modeled by AlphaFold. This surface is colored as a function of the conservation of the residues in HSF2BP homologs, from red (non-conserved) to blue (strictly conserved); conservation scores calculated using ConSurf (50). Three conserved patches are identified: one patch on helix  $\alpha 1$ ; one patch on the armadillo domain and helix  $\alpha 2$ ; one patch on the armadillo domain, at the interface with BRCA2. (B) Interaction of one HSF2BP dimer, displayed as in panel A, with two other HSF2BP dimers, displayed in dark grey, in the HSF2BP-BRCA2 model. Interdimeric contacts are observed between  $\alpha 1$  dimers, an  $\alpha 2$  coiled coil and an armadillo domain, and two  $\alpha 2$  coiled coils. These interfaces are at least partially conserved. (C) Analysis of the electrostatic potential at the surface of a 3D model of the complex formed by 24 HSF2BP molecules, as shown in Fig. 3A. This surface is colored from red (negatively charged) to blue (positively charged). It is mainly negatively charged. All these images were produced using Pymol 2.5.2.

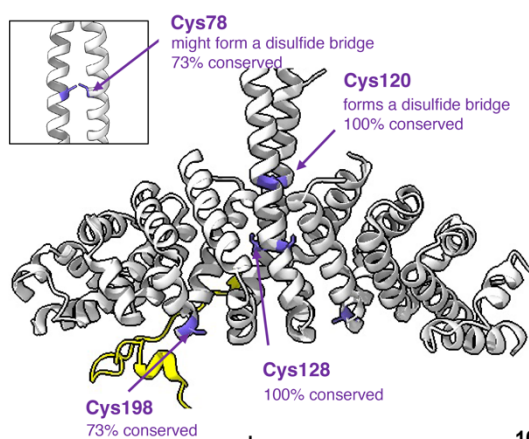


## Supplementary Fig. S9

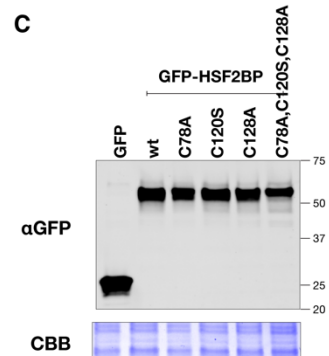
**A**



**B**



**C**



**D**

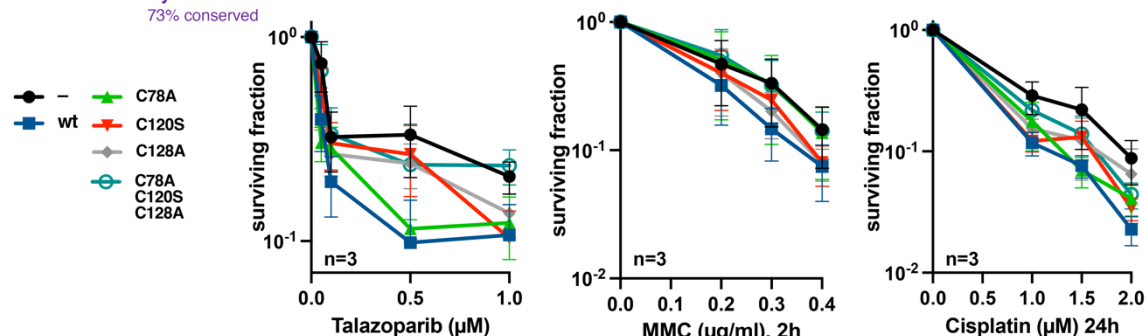


**Fig. S9. Cysteine residues contribute to HSF2BP function.** (A) Sequence alignment of human HSF2BP with ten homologs from mammals to fishes. Positions corresponding to human HSF2BP cysteines are boxed, positions at the interfaces between HSF2BP dimers are labelled with green numbers. (B) Position of the cysteines in the 3D structure of dimeric HSF2BP. The armadillo dimer is shown in the main panel (PDB 7LDG), and part of the helix  $\alpha$ 2 coiled coil is displayed in the black box (AlphaFold model). The BRCA2-HBD peptide is in yellow. The cysteines are in purple. (C) SDS-PAGE gels of the GFP-HSF2BP variants expressed in HeLa cells. (D) Survival assays performed with cells expressing the single cysteine mutants C78A, C120S and C128A, as well as the triple mutant combining the three mutations.

**Table S1. Data collection and SAXS-derived parameters.**

**Data collection parameters**

Radiation source	Synchrotron SOLEIL
Beamline	SWING
Detector	Eiger 4M under vacuum
Wavelength (nm)	0.103
Sample-detector distance (m)	2.0
$s$ range (nm <sup>-1</sup> )	0.03 – 5.7
Exposure time (s)	36 frames of 0.99 s each
Temperature (K)	293.15

**Overall parameters**

Concentration (mg/mL)	1.8 - 2
$R_g$ from Guinier approximation (nm)	$8.50 \pm 0.11$
$R_g$ from PDDF* (nm)	$8.24 \pm 0.05$
Max. Intra-molecular distance $D_{MAX}$ (nm)	25
Porod Volume, $V_P$ (nm <sup>3</sup> )	349.4
Molecular weight, $I(0)$ (kDa)	$156 \pm 21$
Expected molecular weight (e.g. sequence) (kDa)	150

**Software employed**

Primary data reduction	Foxtrot 3.5.2-3645
Data processing	PRIMUS
Modelling	DAMMIN

---

SASBDB

SASDSM7

---

\*Pair distance distribution function

**Table S2. Data collection and refinement statistics related to the crystal structures of HSF2BP helix  $\alpha$ 1 and HSF2BP helix  $\alpha$ 1 bound to BRME1-M.**

	HSF2BP- $\alpha$ 1	HSF2BP- $\alpha$ 1 / BRME1-M
<b>Data collection</b>		
Space group	$P 4_3 3 2$	$I 4_1 2 2$
Cell dimensions		
$a, b, c$ (Å)	79.81, 79.81, 79.81	73.87, 73.87, 92.80
$\alpha, \beta, \gamma$ (°)	90, 90, 90	90, 90, 90
$Za$	2	1:1
Wavelength (Å)	0.96546	0.96546
Resolution (Å)	60.0 - 1.48 (1.52 - 1.48)	36.9 - 1.9 (1.95 - 1.9)
Estimated resolution limit (Å)*	1.48, 1.48, 1.48	2.44, 2.44, 1.71
$R_{pim}$	0.021 (0.565)	0.019 (0.976)
$R_{merge}$	0.050 (1.393)	0.049 (2.384)
$I / \sigma I$	15.0 (1.2)	12.8 (0.7)
$CC_{1/2}$	0.999 (0.559)	0.999 (0.429)
Completeness (%)	99.8 (99.9)	99.6 (99.6)
Redundancy	6.6 (6.8)	6.9 (6.9)
$R_{merge}^*$	0.049 (1.049)	0.041 (0.691)
$I / \sigma I^*$	15.8 (1.6)	20.3 (3.4)
$CC_{1/2}^*$	0.999 (0.610)	0.999 (0.820)
Completeness (%)*	94.9 (50.6)	61.5 (15.6)
<b>Refinement</b>		
Resolution (Å)	56.43 - 1.48 (1.52 - 1.48)	36.9 - 1.9 (2.04 - 1.9)
No. reflections	14159 (430)	6522 (384)
$R_{work} / R_{free}$	21.27/21.66	23.34/24.36
No. non-hydrogen atoms		
Protein	506	551
Ligand/ion	10	38
Water	56	28
$B$ -factors		
Protein	35.8	52.0
Ligand/ion	21.2	86.0
Water	48.0	71.6
R.M.S. deviations		
Bond lengths (Å)	0.008	0.008
Bond angles (°)	0.94	0.88
PDBID	<b>8A50</b>	<b>8A51</b>

Values in parentheses are for highest-resolution shell.

Dataset from one single crystal used per structure.

\*Values calculated after truncation by STARANISO. Estimated resolution limits along the three crystallographic directions  $a^*$ ,  $b^*$ ,  $c^*$ .

**Table S3. Cryo-EM data collection, refinement and validation statistics.**

---

<b>EMD-16432</b>	
<b>Data collection and processing</b>	
Voltage (kV)	300
Electron exposure (e-/Å <sup>2</sup> )	40
Defocus range (μm)	-0.4 to -1.8
Pixel size (Å)	0.73
Symmetry imposed	D3
Initial particle images (no.)	660 000
Final particle images (no.)	398 000
Map resolution (Å)	3.26
FSC threshold	0.143
Map resolution range (Å)	3-8

---



***Data S1***

Excel file containing numerical data plotted in the main and the supplementary figures.